



HAL
open science

Investigating the role of geology in the hydrological response of Mediterranean catchments prone to flash-floods: regional modelling study and process understanding

O. Vannier, Sandrine Anquetin, Isabelle Braud

► To cite this version:

O. Vannier, Sandrine Anquetin, Isabelle Braud. Investigating the role of geology in the hydrological response of Mediterranean catchments prone to flash-floods: regional modelling study and process understanding. *Journal of Hydrology*, 2016, 541 (Part A), pp.158-172. 10.1016/j.jhydrol.2016.04.001 . hal-02604838

HAL Id: hal-02604838

<https://hal.inrae.fr/hal-02604838>

Submitted on 16 May 2020

HAL is a multi-disciplinary open access archive for the deposit and dissemination of scientific research documents, whether they are published or not. The documents may come from teaching and research institutions in France or abroad, or from public or private research centers.

L'archive ouverte pluridisciplinaire **HAL**, est destinée au dépôt et à la diffusion de documents scientifiques de niveau recherche, publiés ou non, émanant des établissements d'enseignement et de recherche français ou étrangers, des laboratoires publics ou privés.

1 Investigating the role of geology in the hydrological response of
2 Mediterranean catchments prone to flash-floods: regional
3 modelling study and process understanding

4 Olivier Vannier^{a,*}, Sandrine Anquetin^{a,b}, Isabelle Braud^c

5 ^a *Université Grenoble Alpes, LTHE, Grenoble Cedex 9, France*

6 ^b *CNRS, LTHE, Grenoble Cedex 9, France*

7 ^c *IRSTEA, UR HHLV (Hydrology-Hydraulics), Villeurbanne Cedex, France*

8 **Abstract**

9 In this study, a regional distributed hydrological model is used to perform long-
10 term and flash-flood event simulations, over the Cévennes-Vivarais region (south
11 of France). The objective is to improve our understanding on the role played by
12 geology on the hydrological processes of catchments during two past flash-flood
13 events. This modelling work is based on Vannier et al. (“Regional estimation of
14 catchment-scale soil properties by means of streamflow recession analysis for use in
15 distributed hydrological models”, *Hydrological Processes*, 2014), where streamflow
16 recessions are analysed to estimate the thickness and hydraulic conductivity of
17 weathered rock layers, depending on the geological nature of catchments. Weath-
18 ered rock layers are thus implemented into the hydrological model CVN-p, and
19 the contribution of these layers is assessed during flash-flood events simulations
20 as well as during inter-event periods. The model is used without any calibration,
21 to test hypotheses on the active hydrological processes. The results point out
22 two different hydrological behaviours, depending on the geology: on crystalline
23 rocks (granite and gneiss), the addition of a weathered rock layer considerably
24 improves the simulated discharges, during flash-flood events as well as during re-
25 cession periods, and makes the model able to remarkably reproduce the observed

26 streamflow dynamics. For other geologies (schists especially), the benefits are
27 real, but not sufficient to properly simulate the observed streamflow dynamics.
28 These results probably underline the existence of poorly known processes (flow
29 paths, non-linear spilling process) associated with the planar structure of schisty
30 rocks. On a methodological point of view, this study proposes a simple way to
31 account for the additional storage associated with each geological entity, through
32 the addition of a weathered porous rock layer situated below the traditionally-
33 considered upper soil horizons, and shows its applicability and benefits for the
34 simulation of flash flood events at the regional scale.

35

36 *Keywords:* hydrological modelling, process understanding, flash-floods, geology,
37 regional modelling

38 1. Introduction

39 In the field of catchment hydrology, many efforts are made to better un-
40 derstand the climate and landscape controls on the water cycle and catchments
41 response dynamics. This thirst of knowledge is largely related to the most chal-
42 lenging problem that has driven the hydrologic community researches for the last
43 decade: predicting the response of ungauged catchments. This challenge, concep-
44 tualized within the PUB initiative (Sivapalan *et al.*, 2003), has resulted in a large
45 amount of recent hydrological studies, as reviewed by Hrachowitz *et al.* (2013),
46 focusing on crucial questions such as process understanding (Tetzlaff *et al.*, 2007;
47 Blume *et al.*, 2008, for example), catchments classification (Sawicz *et al.*, 2011,

*Corresponding author

Email address: oliviervannier@gmail.com (Olivier Vannier)

48 among many), uncertainty analyses (McMillan *et al.*, 2010, e.g.), model param-
49 eter transferability (Oudin *et al.*, 2010, e.g.) or emerging observation techniques
50 (Selker *et al.*, 2006). Even if progress still need to be made to reach the ambitious
51 target defined in the PUB initiative, significant advances have been made in the
52 field of regionalisation methods (Parajka *et al.*, 2005; Oudin *et al.*, 2008; Parajka
53 *et al.*, 2013; Salinas *et al.*, 2013, e.g.) and emerging modelling approaches (Fenicia
54 *et al.*, 2008a,b; Savenije, 2010; Clark *et al.*, 2011).

55

56 Among the dominant factors driving the hydrological behaviour of catchments,
57 geology is regularly cited as an important one (Yadav *et al.*, 2007; Tetzlaff *et al.*,
58 2007; Oudin *et al.*, 2010, e.g.). At the catchment scale, geology affects the govern-
59 ing hydrological processes through many ways, such as (for example): i) ground-
60 water flow paths direct implication on the transit time distribution of water within
61 catchments (Sayama & McDonnell, 2009; Rinaldo *et al.*, 2011); ii) the nature of
62 the interface between soil horizons and bedrock determining the formation of
63 preferential flows that governs the quick response during flood events (Weiler &
64 Naef, 2003; Weiler & McDonnell, 2007); iii) bedrock permeability strongly impact-
65 ing the water balance at the catchment scale (Tromp-van Meerveld *et al.*, 2007).
66 More generally, we consider that geology is directly linked to the catchments wa-
67 ter storage capacity, which has been shown to be of primary importance in the
68 water cycle dynamics (Sayama *et al.*, 2011; Tetzlaff *et al.*, 2011; McNamara *et al.*,
69 2011) and which strongly influences the antecedent wetness conditions that acts
70 as a threshold on the response of catchments during flood events (Troch *et al.*,
71 2003; Latron & Gallart, 2008; Zehe *et al.*, 2010).

72

73 To better understand the role played by landscape characteristics in the hy-

74 drological behaviour of catchments, distributed hydrological modelling appears as
75 a very relevant tool (Vivoni *et al.*, 2007; Noto *et al.*, 2008; Anquetin *et al.*, 2010;
76 Braud *et al.*, 2010; Nester *et al.*, 2011; Garambois *et al.*, 2015). As mentioned
77 by Parajka *et al.* (2013), besides all the efforts recently made to better estimate
78 and regionalize model parameters, there is a real need for improving the model
79 structures to better understand and reproduce the active hydrological processes.
80 In that way, recent developments made around flexible, data-driven and evolu-
81 tive modelling approaches (Fenicia *et al.*, 2011; Kavetski & Fenicia, 2011; Gharari
82 *et al.*, 2014) appear as very promising.

83

84 In the work presented here, we pursue the multiple working hypotheses ap-
85 proach advocated by Clark *et al.* (2011). The modelling process followed here
86 consists in a "Try - Fail - Learn - Repeat" iterative methodology used for test-
87 ing hydrological functioning hypotheses, and making the best use of what data
88 can teach (Fenicia *et al.*, 2008a). The objective of this distributed hydrological
89 modelling study is to better assess the role played by geology in the different hy-
90 drological behaviours observed in the Cevennes-Vivarais region (Mediterranean
91 area), located in the south of France. The catchments of this region are prone to
92 flash-floods, which represent the most destructive hazard in the mediterranean
93 region (Gaume *et al.*, 2009). Consequently, the hydrological response of the
94 Cevennes-Vivarais catchments to flood events have long been observed, within
95 the Cevennes-Vivarais Hydro-Meteorological Observatory¹ (Boudevillain *et al.*,
96 2011), and subject of many hydrological modelling studies (Le Lay & Saulnier,
97 2007; Bonnifait *et al.*, 2009; Garambois *et al.*, 2013, e.g.). Several works aiming

¹<http://www.ohmcv.fr>

98 at developing and assessing forecast tools and flash-flood warning systems also
99 focus on the Cevennes-Vivarais region (Bouilloud *et al.*, 2010; Vincendon *et al.*,
100 2010; Alfieri *et al.*, 2011), or on neighbouring french mediterranean regions like the
101 Var department, hit by massive floods in June 2010 (Javelle *et al.*, 2014; Caseri
102 *et al.*, 2015). However, the purpose of the current work significantly diverges
103 from forecast-oriented studies, in the sense that it is governed by the understand-
104 ing of unknown processes, instead of the will to obtain the best results as possible.

105

106 Recently, the FloodScale reasearch project² (Braud *et al.*, 2014), which is a
107 contribution to the international HyMeX program³, has been federating the french
108 hydrologic community on research questions related to the understanding and
109 simulation of the hydrological processes leading to flash floods in mediterranean
110 catchments. Here, we use the CVN-p process-oriented distributed model, deriving
111 from CVN (Manus *et al.*, 2009), set-up over the entire Cevennes-Vivarais region,
112 and accounting for evapotranspiration and vegetation-related processes to perform
113 continuous simulations. This study follows the works of Vannier *et al.* (2014),
114 who analysed observed streamflow recession curves and derived catchment-scale
115 aquifer effective thicknesses and hydraulic conductivity, for the different geological
116 entities of the region, using the approach proposed by Brutsaert & Nieber (1977).
117 Here a weathered porous rock layer is added in the model, to fill the lack of water
118 storage capacity identified when considering soil horizons only (Roux *et al.*, 2011;
119 Vannier *et al.*, 2014; Garambois *et al.*, 2015).

120

121 The paper is organized as follows. We first describe the model used in this

²<http://floodscale.irstea.fr>

³<http://www.hymex.org>

122 study and, in section 3, how the CVN-p hydrological model is set-up over the
123 study area. In the fourth section we present the results of the simulations per-
124 formed with and without the addition of the weathered porous rock layer, and
125 we evaluate the model performances obtained for year 2008, with a focus on two
126 flood-events that occurred during the autumn. Subsequently, we discuss the results
127 obtained and the observed spatial differences in the model performances, in link
128 with the geology of catchments ('Discussion' section). The final section consists of
129 brief conclusions and of some perspectives for future developments on this subject.

130

131 **2. Model description**

132 The model used in this study is the CVN-p hydrological model. The CVN-p
133 model is an evolution of the event-based rainfall-runoff model CVN (Manus *et al.*,
134 2009). Several processes have been implemented in the model so that it can run
135 long-term continuous simulations.

136

137 *2.1. Structure and processes represented*

138 The CVN-p model was built within the LIQUID hydrological modelling plat-
139 form (Viallet *et al.*, 2006; Branger *et al.*, 2010), which is a framework providing
140 users the possibility to assemble hydrologic modules together, each one solving a
141 physical process. In its early version, CVN was an event-based model, represent-
142 ing two main processes: the vertical water transfer through soils, and the routing
143 of the generated runoff along the hydrographic network (Manus *et al.*, 2009).

144

145 For the regional simulation purposes, the model evolved to perform continuous
 146 simulations. Root extraction, vegetation growth, interception and evapotranspi-
 147 ration processes were added, in order to simulate a realistic water balance and get
 148 a dynamic evolution of soil wetness. The box-type structure of the model CVN-p,
 149 with the implemented modules and their inter-connexions is given and compared
 150 to the previous CVN version in Fig.1. A detailed description of the different hy-
 151 drological modules coupled within the continuous CVN-p model is presented in
 152 Appendix A.

153 The model is forced with two spatialised variables : precipitation and reference
 154 evapotranspiration (ET_0). Precipitation is necessarily liquid (the model does not
 155 account for snow accumulation nor melting). Forcings are interpolated over the
 156 model mesh using weighted averages by a dedicated module (INPUT).

157

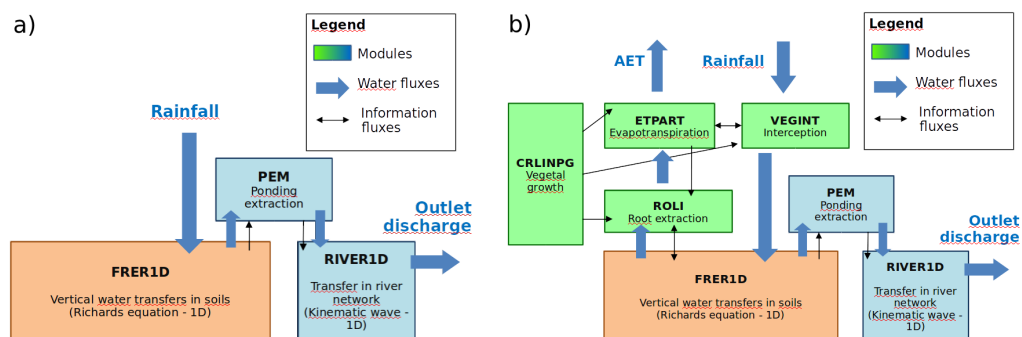


Figure 1: Structure of the event-based model CVN (Manus *et al.*, 2009; Anquetin *et al.*, 2010; Braud *et al.*, 2010) (a) and the continuous model CVN-p used in this study (b). The modules are coloured according to the type of process: brown for the soil compartment, blue for runoff and river flow, and green for the vegetation-related processes.

158 2.2. Spatial discretization

159 The CVN-p model spatial discretization is based on the Representative Ele-
 160 mentary Watershed approach (REW) (Reggiani *et al.*, 1998, 1999) later adapted

161 by Dehotin & Braud (2008) who proposed the “hydrolandscape” concept used here.
162 An hydrolandscape is an elementary hydrological response unit, homogeneous in
163 terms of hydrological processes. In this study, following the approach of Manus
164 *et al.* (2009), we assume that topography and soil typology represent the dom-
165 inant control processes on the Cevennes-Vivarais region hydrological behaviour.
166 Accordingly, the hydrolandscapes are defined as the crossing of two successive
167 discretization steps: i) first the study domain is splitted into sub-catchments
168 using an automated DEM-based tool (Tarboton, 1997), with a threshold of 0.5
169 km²; ii) then a second level of discretization is applied, using a pedological soil
170 map. The dominant vegetation type is finally assigned to each hydrolandscape.
171 The hydrolandscapes are the elementary cells of the soil and vegetation processes
172 solved by the CVN-p model. The river network, where runoff extracted from each
173 hydrolandscape is sent and routed, is extracted from the DEM analysis: each sub-
174 catchment is associated to a river reach.

175

176 *2.3. Implementation of a weathered rock layer*

177 Vannier *et al.* (2014) proposed a methodology to define catchment-scale -
178 deep - soil properties through the analysis of streamflow recession data, based
179 on the works of Brutsaert & Nieber (1977). They performed this analysis after
180 they lacked information on the physical (thickness) and hydraulic (conductivity)
181 properties of weathered rock layers, which stands below well-described upper-soil
182 horizons (Fig.2a).

183

184 The application of the streamflow recession analysis over a sample of catch-
185 ments, located in the Cevennes-Vivarais region (south of France), highlighted a

186 strong link between the dominant geology and the estimated values of the thick-
 187 ness and hydraulic conductivity of these deep horizons (Fig.2b). Values of sat-
 188 urated hydraulic conductivities presented in Fig.2b can be seen as very large,
 189 and thus out of the range of standard values of conductivities reported for soils
 190 or porous rocks. This is due to the nature of the values characterized by Van-
 191 nier *et al.* (2014): first, the presence of various poorly-known processes such as
 192 macroporosity, rock fracturing, or preferential flow directions, may result in flow
 193 conditions that significantly diverge from the theory, and in addition, these val-
 194 ues are representative of catchment-wide integrated processes since they derive
 195 from streamflow recession analyses. Consequently, values reported in Fig.2b must
 196 rather be considered as “effective” parameters than as actual hydraulic conduc-
 197 tivities.

198

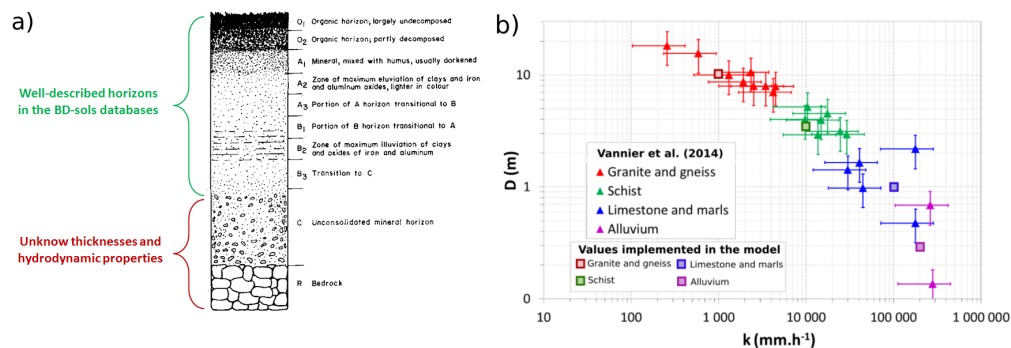


Figure 2: Figures adapted from Vannier *et al.* (2014) : a) Typical pedologic profile, after Kang & Tripathi (1992) and level of description in the Cevennes-Vivarais BD-sols soil databases. b) Depth to bedrock D and lateral hydraulic conductivity k calculated using streamflow recession analysis. The confidence intervals result from the uncertainty in the value of drainable porosity (between $0.05 \text{ m}^3 \cdot \text{m}^{-3}$ and $0.1 \text{ m}^3 \cdot \text{m}^{-3}$). Values implemented (Table 1) have been added to the figure.

199 In the present paper, we propose to implement deep weathered rock layers into
 200 the CVN-p hydrological model to perform simulations over the Cevennes-Vivarais
 201 region. The thickness and hydraulic conductivity of such layers are directly taken

	Thickness D (m)	Saturated water content	Saturated hydraulic conductivity K_s (mm.h ⁻¹)
Granite and gneiss	10	0.1	1 000
Schist θ_s (m ³ .m ⁻³)	3.5	0.1	10 000
Limestone	1	0.1	100 000
Alluvium	0.2	0.1	200 000

Table 1: Chosen values of thickness and saturated hydraulic conductivity of deep weathered rock horizons, according to the dominant geology.

202 from the results obtained by Vannier *et al.* (2014): an average value of these pa-
203 rameters is considered for each of the four dominant rock types present in the
204 region (Table 1). Implementing additional layers is easy in the CVN-p model, as
205 the FRER1D module can account for different horizons with their own hydraulic
206 properties.

207

208 2.4. Boundary conditions

209 A free gravitary flux condition is used at the bottom of the vertical soil +
210 weathered rock columns, so that water can percolate according to a unitary gra-
211 dient of charge. The percolation flux is then directly sent into the nearest river
212 reach, similarly to the extracted ponding flux. This free bottom boundary con-
213 dition of the CVN-p model (here -p stands for “percolation”) is one of the main
214 differences with the CVN model used by Manus *et al.* (2009); Anquetin *et al.*
215 (2010); Braud *et al.* (2010), in which a null flux condition was used.

216

217 Coupled to the implementation of weathered rock layers, the use of a grav-
218 itary bottom flux condition sent into the river network represents a conceptual
219 way to account for a delayed groundwater flow term simulated in the model. The

220 transit-time of water through the entire column depends on its thickness, hy-
221 draulic conductivity and wetness state.

222

223 **3. Regional set-up of the model**

224 *3.1. Presentation of the area and available data*

225 The CVN-p model is set-up over the seven largest catchments in the Cevennes-
226 Vivarais region : the Ardèche (2263 km²) Cèze (1372 km²) and Gardon (1914
227 km²) catchments at their confluence with the Rhône river, the Vidourle at Som-
228 mières(650 km²), the Vistre at its confluence with the Rhony river (493 km²), the
229 Hérault at Gignac (1410 km²) and the Tarn at Montbrun (589 km²) rivers. The
230 location of these catchments is shown on the map in Fig. 3, as well as the geology
231 of the region and the location of the stream gauges.

232

233 The Digital Elevation Model (DEM) used for the discretisation procedure is
234 the 25m-resolution DEM provided by the french National Geographic Institute
235 (IGN). Soil data are provided by the BD-sols Ardèche and Languedoc-Roussillon
236 spatial databases (Robbez-Masson *et al.*, 2000). These pedological databases pro-
237 vide information on the dominant soil units (1:250 000 scale), as well as on the
238 physical properties (texture, structure) of the main soil types that compose these
239 units.

240

241 Spatial vegetation information required for the computation of interception
242 and evapotranspiration processes derives from the Corine Land Cover (2006)
243 public database. Monthly average values of LAI, crop coefficients, as well as

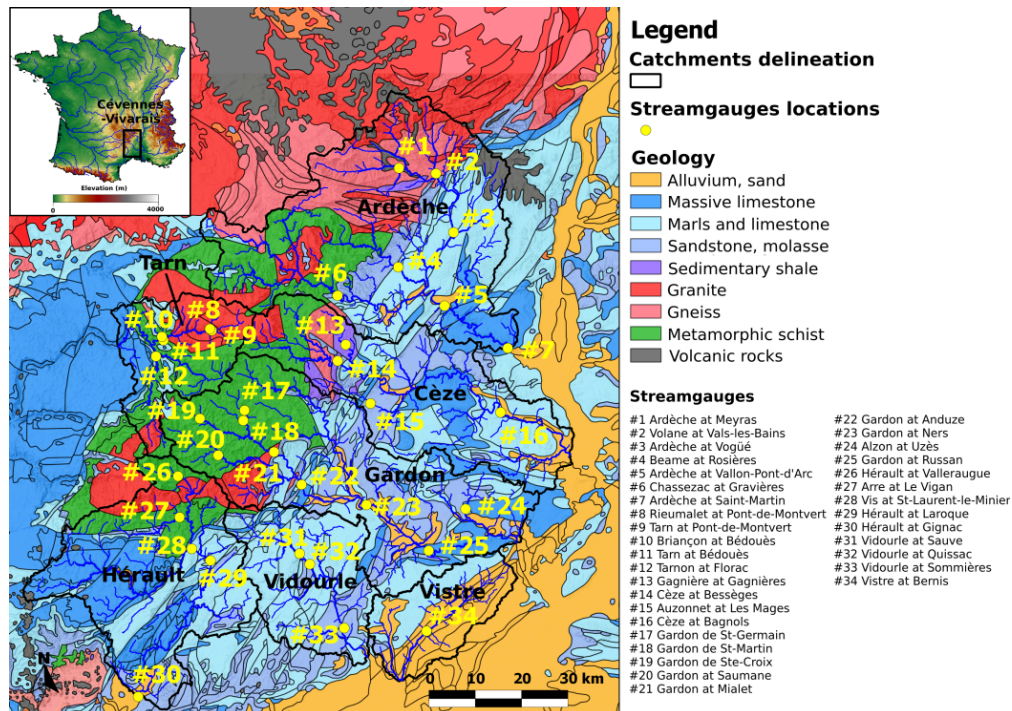


Figure 3: Location of the seven selected catchments, and dominant geology of the Cévennes-Vivarais region (deriving from the 1:1 000 000 french geological map). The location of the streamgauges from which measurements are used in this study is symbolized by yellow points.

244 root depths of different types of vegetation are extracted from the ECOCLIMAP
 245 database (Masson *et al.*, 2003). Geology derives from the 1:1 000 000 scale na-
 246 tional geological map⁴.

247

248 3.2. Forcings

249 The set-up of the CVN-p model requires different kinds of data. Meteoro-
 250 logical forcings are rainfall and reference evapotranspiration ET_0 . For inter-
 251 events periods, rainfall data is extracted from SAFRAN meteorological reanalyses
 252 (Quintana-Seguí *et al.*, 2008; Vidal *et al.*, 2010), whereas for events simulation we

⁴<http://www.brgm.fr>

253 use kriged hourly raingauges measurements. ET_0 is computed on the basis of
254 other meteorological variables provided by SAFRAN (temperature, wind speed,
255 long and short-wave radiation, specific air humidity). The Penman-Monteith for-
256 mulation (Monteith, 1965) is used, with parameters values chosen according to the
257 Food and Agricultural Organization (FAO) recommandations (Allen *et al.*, 1998).

258

259 The input forcing variables are given on spatial grids, with a resolution varying
260 from $8 \times 8 \text{ km}^2$ (SAFRAN meteorological reanalyses) to $1 \times 1 \text{ km}^2$ (hourly kriged
261 rainfall products). The temporal resolution is 1 hour, even if in the case of
262 SAFRAN, rainfall intensities have been shown to be slightly biased at this tem-
263 poral resolution (see Vidal *et al.* (2010) for more details).

264

265 3.3. Parameters specification

266 The modelling approach used in this study is based on the testing of hydrolog-
267 ical functioning hypotheses, without any calibration of the model. Consequently,
268 parameters values derive from an *a priori* knowledge provided by observations,
269 maps, and available databases. As an example, soil hydraulic properties required
270 within the Brooks & Corey (1964) relationships (FRER1D module) are computed
271 according to the Rawls & Brakensiek (1985) pedotransfer function, using struc-
272 tural and textural information given by the BD-sols databases. Other parameters
273 values can be directly given by databases (Vegetation parameters), or result from
274 regional observations analyses (river geometry, weathered rock horizons proper-
275 ties).

276

277 *3.4. Simulations strategy*

278 In this region, rainfall-runoff simulations are performed over the entire 2008
279 year. The choice of year 2008 was made for two main reasons :

280

281 a) Two major rainfall events occurred during the autumn : the first one between
282 October 21th and October 23rd, and the second one between October 31th
283 and November 5th. These two events affected different areas, and also differ
284 each other by intensity and duration, as shown in Fig.4: the first event is
285 characterized by a shorter duration (approximately 24 hours) and high rainfall
286 intensities (up to several tens of mm per hour) while the second event lasted
287 for more than one day, with lower rainfall rates.

288

289 b) The large availability of discharge data measured by the streamgauges of the
290 region in 2008, as compared to other years. In 2008, almost all of the stream-
291 gauges worked correctly, even during flood events.

292

293 The whole 2008 year is simulated, split into four periods for which rainfall
294 forcings differ (Table 2). Long-term (i.e. inter-events) simulations are performed
295 with SAFRAN rainfall, while events simulations are forced with hourly kriged
296 rainfall fields. The final state of a long-term simulation (soil wetness, water level
297 in the river) is used as initial state of the following event simulation.

298

299 *3.5. Evaluation of the simulations*

300 When complete measured hydrographs are available, an evaluation of the
301 model performance through the calculation of four score indices is performed.

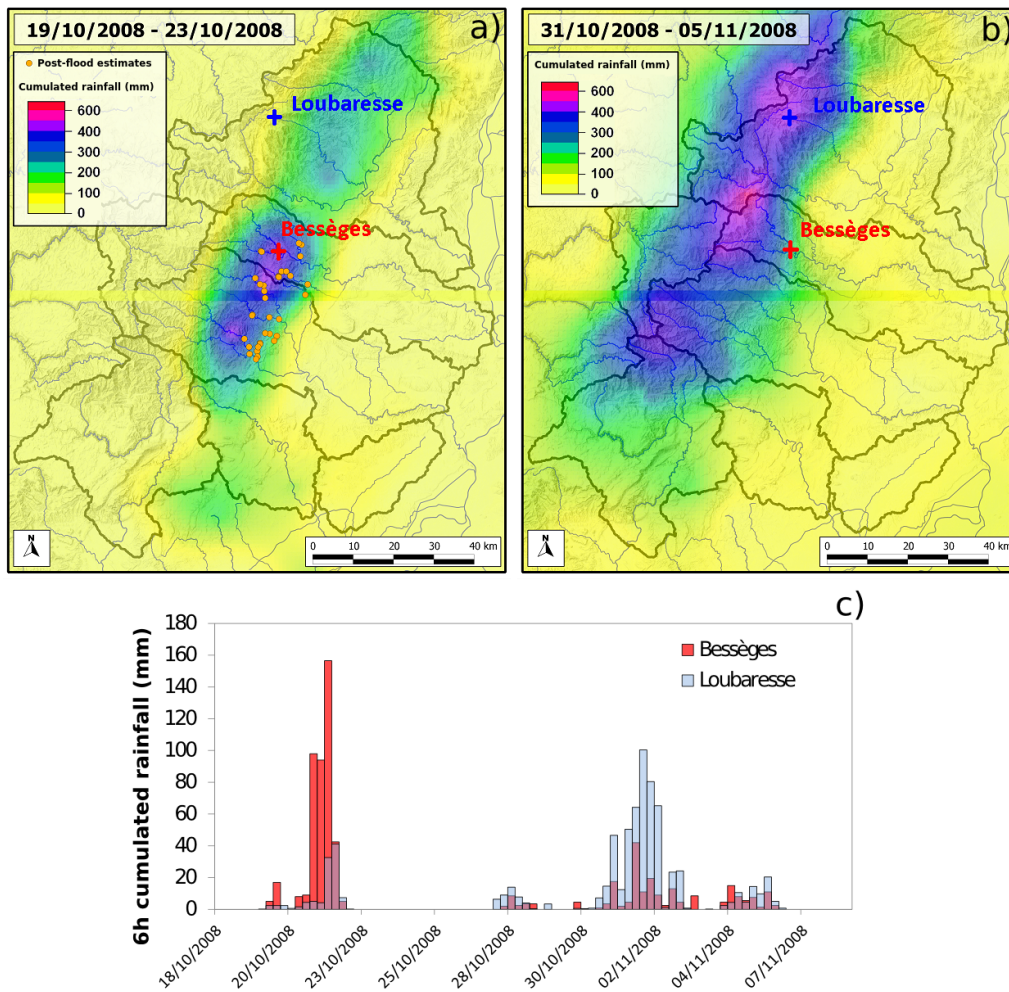


Figure 4: Maps of the cumulated rainfall amounts observed over the Cevennes-Vivarais region during the October 21 - October 23, 2008 event (a) and the October 31 - November 5, 2008 event (b). These maps represent the cumulated rainfall measured on raingauges interpolated through a kriging technique over a 1x1 km² resolution grid. The blue and red crosses indicate the location of the Bessèges and Loubaresse raingauges, for which the measured hyetograms are shown in (c).

Temporal window	Type of simulation	Rainfall forcing
01/01/2008 - 21/10/2008	Initialisation	SAFRAN
21/10/2008 - 23/10/2008	Event	Kriged rainfall
23/10/2008 - 31/10/2008	Transition	SAFRAN
31/10/2008 - 05/11/2008	Event	Kriged rainfall

Table 2: Simulation table

302 Nash-Sutcliffe efficiency (Nash & Sutcliffe, 1970) (NSE), Nash-Sutcliffe efficiency
303 of the logarithmic discharge (LNSE), correlation coefficient R^2 and bias indicator
304 PBIAS (Kling & Gupta, 2009) are computed. Along with the traditional perfor-
305 mance indices computation, a deep attention is paid to visual comparison between
306 observed and simulated hydrographs, to evaluate the model ability to reproduce
307 catchments response. Visual comparison is complementary to quantitative evalu-
308 ation, in a sense that it gives indications on the ability of the model to reproduce
309 flow dynamics, recession rates or flood timing, which are not easily summarised in
310 score indices. In addition, visual evaluation allows the distinction between time
311 periods where the model gives good results, and periods where it is not the case,
312 and thus makes the interpretation of the results easier.

313

314 *Long-term simulations*

315

316 In order to assess the role of the added weathered rock layer, same simulations
317 are done with and without weathered rock layer. This evaluation is performed on
318 several catchments of different sizes: three Tarn sub-catchments, essentially com-
319 posed of granites and gneiss (the Rieumalet, the Tarn at Pont-de-Montvert, and
320 the Tarn at Bedouès, #8, #9 and #11, respectively, in Fig.3); and five Gardon

321 sub-catchments, where schists are dominant on the upper part while sedimentary
322 rocks mainly cover the downstream part (Gardon at Saint-Martin, Mialet, An-
323 duze, Ners and Russan, #18, #21, #22, #23 and #25, respectively, in Fig.3).
324 Compared discharge series begin on April 1, 2008 and end on October 21, 2008.
325 In these simulations the three first months are ignored (simulations effectively
326 start on January 1, 2008) in order to avoid initialisation artefacts. Sensitivity
327 tests (not shown here) were performed to assess the average necessary spin-up
328 duration, and a value of three months appeared as enough in the large majority
329 of cases;

330

331 *Event simulations*

332

333 The contribution of the implemented weathered rock layer is assessed in the
334 same way during flood events, for the same selected catchments. For each catch-
335 ment, the considered event is the one which caused the largest observed hydrologic
336 response (highest discharge values).

337

338 At the regional scale, the evaluation of the event simulations is performed for
339 a wide range of catchment sizes, for which two types of observations are available:

340

341 a) Peak discharge estimated *a posteriori* in 35 catchments, ranging from 1 to 100
342 km², during the post flood investigation of the October 21-23 event. The post
343 flood survey follows the methodology defined by Gaume & Borga (2008);

344

345 b) Discharge measurements, available on 34 operationnal streamgauges in the re-

346 gion, for catchment sizes ranging from 30 to 2300 km². Discharge values derive
347 from automatic water level devices recording at variable timestep. A record is
348 made for each variation of water level larger than a defined threshold (which
349 is specific to each station).

350

351 Along with these direct comparison to observations, event simulations results
352 are also compared at the regional scale to CRUPEDIX 10-years return period
353 discharge estimates. Q_{10} is computed according to equation 1, after the CRU-
354 PEDIX formula (1980), which is an empirical estimation of the instantaneous
355 10-years return period peak discharges for catchment size lower than 2000 km².

$$Q_{10} = A^{0.8}(P_{d10}/80)^2C \quad (1)$$

356 where Q_{10} is the 10-years return period instantaneous peak discharge (m³.s⁻¹);
357 A is the catchment area (km²); P_{d10} the 10-years return period daily rainfall
358 depth for the considered catchment (mm), and C is a regional coefficient (with a
359 dimension of [T⁻¹.L^{-0.6}]), here considered equal to 1.7 (Versini *et al.*, 2010). The
360 estimation of the P_{d10} rainfall for all the considered catchments is based on the
361 grided SAFRAN meteorological reanalyses: an estimation of the 10-years return
362 period daily rainfall is performed for each SAFRAN grid cell according to its
363 statistical distribution. Then the areal rainfall for each catchment is computed
364 through the aggregation of all the values affected to the SAFRAN grid cells con-
365 tained within the considered catchment, and the use of an Areal Reduction Factor
366 (ARF) (De Michele *et al.*, 2001), with specific coefficient values for the Cevennes-
367 Vivarais region (Ceresetti, 2011). Due to its simplicity, the CRUPEDIX method
368 does not provide a perfectly accurate estimation of the 10-years return period peak

369 discharge. We performed a comparison (not shown here) between CRUPEDIX
370 estimates and data-based 10-years return period peak discharge obtained by fit-
371 ting annual maxima to a Gumbel distribution, on all streamgauges of the region.
372 It showed a globally fair agreement, despite a tendency of CRUPEDIX to overes-
373 timate 10-years return period peak discharges on small catchments ($< 200 \text{ km}^2$).
374 Note that a more recent method, named SHYREG (Aubert *et al.*, 2014), has
375 been developed for the estimation of reference peak discharge in mediterranean
376 catchments. But the homogeneous application of the CRUPEDIX method over
377 the whole study area, even on ungauged streams, allows its use as a common
378 reference for the evaluation of regional flood discharges. Consequently, the ratio
379 Q_{max}/Q_{10} , where Q_{max} is the maximum simulated peak discharge, gives a clear
380 indication of the simulated severity of the flood, on each reach of the hydrographic
381 network.

382

383 4. Results

384 4.1. Contribution of the implemented weathered rock layer

385 The contribution of the implementation of a weathered rock layer in the model
386 is assessed through a comparison between measured discharge and simulated dis-
387 charge obtained with and without the weathered rock layer. Results are compared
388 and analysed for each geology type. Tables 3 and 4 summarise the scores obtained
389 for each simulation.

390 4.1.1. Granite and gneiss

391 On crystalline rock (granite and gneiss) catchments located on the Tarn river,
392 the benefits of including a deep weathered rock layer are clear, whether for event or

393 long-term simulations. For long-term simulations, adding a deep weathered rock
394 horizon significantly increases the Nash-Sutcliffe efficiency and the Nash-Sutcliffe
395 efficiency of the logarithmic discharge (Table 3), which turns from negative to
396 better than 0.7 values on each of the three catchments. R^2 criteria values also
397 improve in all cases. One must notice a slight increase of the PBIAS index values
398 (becoming positive in all cases) when adding the weathered rock layer. For event
399 simulations, results are also improved when adding the deep weathered rock hori-
400 zon (4): on each of the catchments, the four performance indicators get better
401 values when adding the deep layer. Especially, Nash-Sutcliffe efficiency of the
402 logarithmic discharge and PBIAS index reach satisfying values for non-calibrated
403 event simulations (Table 4).

404

405 As an example, Fig.5a compares the measured and the two simulated hy-
406 drographs (one with and one without the weathered rock layer) on one of the
407 granitic catchments (Tarn at Pont-de-Montvert, #9) during several months. The
408 visual improvement of the model's behavior when using the weathered rock layer
409 is very significant. The model version in which there is no weathered rock layer
410 produces a noisy discharge signal during long-term simulations, corresponding to
411 a direct response to the precipitation signal. When adding the weathered rock
412 layer, the long-term simulated discharge signal is smoother: the layer acts as a
413 buffer, delaying the hydrologic response in time. This behavior is very similar
414 to the observed response, and the model in this version reproduces very well the
415 streamflow dynamics of the granitic catchment. In Fig.5b, the same comparison
416 during the November, 2008 event is shown. Once again, the visual improvement
417 when using the weathered rock layer is clear. While the simulated volume and
418 peak discharge are overestimated by the unmodified model version, the addition

419 of the weathered rock layer brings the simulated hydrograph much closer to the
420 observation. The reason probably stands in the additionnal storage capacity im-
421 plemented in the model: the added weathered rock layer stores a significant part
422 of the infiltrated water, and releases it progressively. On the other hand, the
423 model without additional layer overreacts to precipitation forcings because of its
424 lack of storage: in this case water quickly percolates and almost instantaneously
425 enters the stream network.

426

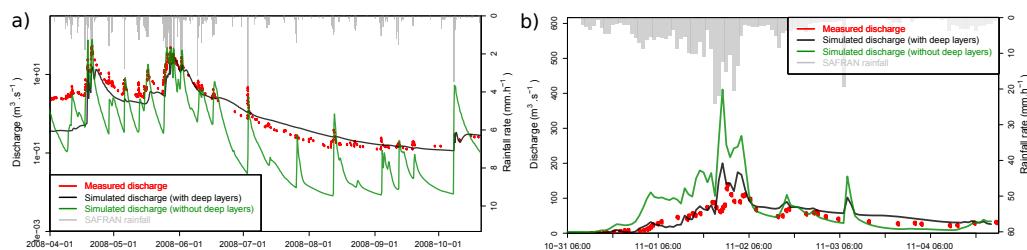


Figure 5: Comparison of measured discharge and discharge simulated by the CVN-p model with and without deep weathered rock layer on a granitic catchment: Tarn in Pont-de-Montvert (67 km^2). a) long-term simulation between April 1, 2008 and October 21, 2008 (discharge scale is logarithmic). b) Event simulation between October 31, 2008 and November 5, 2008.

427 4.1.2. Metamorphic schists and sedimentary rocks

428 On the Gardon river catchments, the dominant geology is composed of meta-
429 morphic schists on the upper part, and limestone and other sedimentary rocks
430 (marls, sandstone) on the lower part. The long-term simulation results are evalu-
431 ated in Table 3 and the scores obtained for the October, 2008 event are shown in
432 Table 4. In this case, the benefits of adding a weathered rock layer in the model
433 are not as important as in the case of granitic catchments. Even if almost all of
434 the performance criteria values increase significantly when adding the layer, this
435 is not sufficient to reach what can generally be considered as “good” performance.
436 Especially, Nash-Sutcliffe values computed on discharge and logarithmic discharge

437 stay closer from 0 than 1 in most of the case. This is particularly true for the
438 event simulation, for which negative Nash-Sutcliffe efficiencies are obtained. Nev-
439 ertheless, correlation coefficients R^2 larger than 0.7 are obtained for long-term
440 simulations.

441

442 A visual evaluation of the model performances gives indications on the causes
443 of such poor performances. As an example, Fig.6 compares the measured and the
444 two simulated hydrographs on the Gardon at Mialet (220 km²), which is a schist-
445 dominated catchment. For the long-term simulation (Fig.6a), the implementation
446 of a weathered rock layer reduces the tendency of the model to simulate frequent
447 variations in the series. This result is similar to the effect observed for granitic
448 catchments, but in this case the smoothing effect due to the weathered rock layer
449 is not sufficient to reproduce satisfyingly the observed discharge series. Simi-
450 larly, the benefits of adding the layer for simulating flood events are incomplete
451 (Fig.6b). Once again, the implementation of this weatherd rock layer decreases
452 the simulated water volume and peak discharge, but the simulated hydrograph
453 still remains larger than the observed one by order of magnitudes (PBIAS criteria
454 exceeds 400 % on this catchment). Apparently, the added layer does not store
455 enough water in the case of schists and sedimentary rocks.

456

457 *4.2. Regional simulations of the 2008 events*

458 *4.2.1. Cases of the two flood events*

459 The two 2008 flood events differ significantly, although their magnitudes re-
460 main approximately similar. The simulated hydrological signature of the two
461 events is shown in Fig.7, where the ratio between simulated peak discharge Q_{max}

Catchment	Dominant geology	Area (km ²)	NSE		LNSE		PBIAS		R2	
			No WRL	WRL	No WRL	WRL	No WRL	WRL	No WRL	WRL
Rieumalet (Pont-de-Montvert, #8)	Granite	20	-0.49	0.67	-1.29	0.71	19.60	-25.53	0.36	0.72
Tarn (Pont-de-Montvert, #9)	Granite	67	0.44	0.65	0.24	0.88	2.15	-35.69	0.69	0.75
Tarn (Bedoués, #11)	Granite	189	-0.26	0.80	-3.09	0.88	1.14	-2.20	0.64	0.82
Gardon (Saint-Martin, #18)	Schist	30	-4.14	-0.06	0.18	0.49	105.73	21.39	0.44	0.69
Gardon (Mialet, #21)	Schist	220	-0.18	0.63	-0.47	0.52	-6.66	-11.22	0.52	0.76
Gardon (Anduze, #22)	Schist	543	-4.41	0.18	-0.97	0.41	136.11	49.97	0.54	0.77
Gardon (Neus, #23)	Limestone / Schist	1100	-2.14	0.61	-0.12	0.68	88.77	20.43	0.46	0.75
Gardon (Russan, #25)	Limestone / Schist	1520	-2.14	0.51	NA ¹	NA ¹	94.01	35.86	0.64	0.81

¹ Undefined value because of null values in the measured discharge series

Table 3: Performance indices of the simulations performed on 8 catchments of various geologies between January 1, 2008 and October 21, 2008. The first three months are not taken into account in the score calculations, to avoid initialisation artefacts. This table compares the results obtained by simulations performed without adding any weathered rock layer in the model (“No WRL”), and simulations including these weathered rock layer (“WRL”).

Catchment	Dominant geology	Area (km ²)	NSE		LNSE		PBIAS		R ²	
			No WRL	WRL	No WRL	WRL	No WRL	WRL	No WRL	WRL
Event: 31/10/2008 - 05/11/2008										
Rieumalet (Pont-de-Montvert, #8)	Granite	20	-6.17	0.43	-0.44	0.63	132.63	10.72	0.18	0.59
Tarn (Pont-de-Montvert, #9)	Granite	67	-6.68	0.10	0.28	0.88	117.85	27.84	0.48	0.68
Tarn (Bedouès, #11)	Granite	189	-1.97	0.59	0.22	0.85	108.85	5.28	0.58	0.59
Event: 21/10/2008 - 23/10/2008										
Gardon (Mialet, #21)	Schist	220	-59.76	-25.57	-0.41	0.08	588.51	401.64	0.76	0.90
Gardon (Anduze, #22)	Schist	543	-7.28	-1.69	-1.47	-0.34	290.48	139.86	0.33	0.30
Gardon (Ners, #23)	Limestone / Schist	1100	-22.07	-11.86	-1.41	-0.62	359.58	259.49	0.07	0.17

Table 4: Performance indices of the simulations performed on 6 catchments of various geologies, during two rainfall events of 2008. This table compares the results obtained by simulations performed without adding any weathered rock layer in the model ("No WRL?"), and simulations including these weathered rock layer ("WRL?").

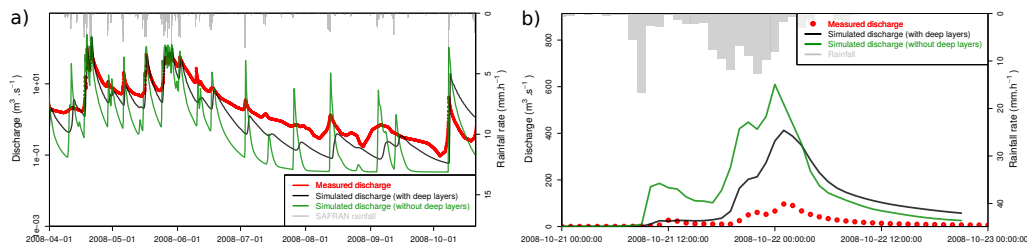


Figure 6: Comparison of measured discharge and discharge simulated by the CVN-p model with and without deep weathered rock layer on a schist catchment: Gardon in Mialet (220 km^2). a) Long-term simulation between April 1, 2008 and October 21, 2008 (discharge scale is logarithmic). b) Event simulation between October 21, 2008 and October 23, 2008.

462 and 10-years return period CRUPEDIX estimated peak discharge Q_{10} (computed
 463 according to equation 1) is presented at the regional scale. Fig.7 highlights the dif-
 464 ferent scales for which the events are the most intense. The October event appears
 465 as intense at all scales, from the smallest catchments ($\sim 1 \text{ km}^2$) located where the
 466 largest rainfall amounts have been observed, to the largest (Cèze, Gardon, Vi-
 467 doure catchments, with an area $> 500 \text{ km}^2$), as the consequence of a routing
 468 effect of the flood. Please note that ratio values computed on small catchments
 469 must be considered carefully, because of the known tendency of CRUPEDIX to
 470 overestimate 10-years return period peak discharges on catchments smaller than
 471 200 km^2 , as mentioned in section 3. On the other hand, the November event is
 472 simulated as very intense only at the largest scales (except one small area located
 473 in the Ardèche catchment), by accumulation effect.

474

475 These differences can be explained by the different natures of streamflow gen-
 476 eration processes simulated by the CVN-p model. Fig.8 presents the map of the
 477 ratio between surface runoff (i.e. overland flow) and delayed groundwater flow
 478 simulated by the CVN-p model for the two events: while massive surface runoff is
 479 simulated by the model during the October event, the November event seems to

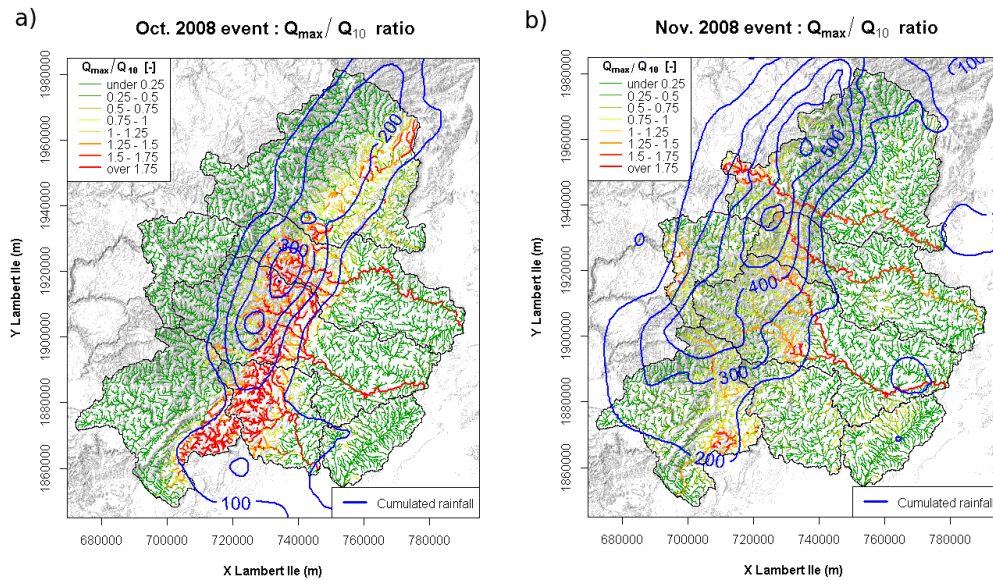


Figure 7: Maps of the ratio between simulated peak discharge Q_{max} and estimated peak discharge Q_{10} of a 10-years return period flood event. The ratio is computed on each river reach. Q_{10} is estimated according to the CRUPEDIX method (1980). a) October 21 - October 23, 2008 event; (b) October 31 - November 5, 2008 event. The contours of the cumulated kriged rainfall amounts appear in blue.

480 be associated with groundwater flow essentially. The areas where surface runoff
 481 is produced during the October event (Fig.8a) spatially match with the zone of
 482 high severity ($Q_{max}/Q_{10} > 1.5$) in Fig.7a. This clearly shows that the simulation
 483 of the October event leads to intense surface runoff, responsible of the severity of
 484 the flood.

485

486 Two reasons probably explain why surface runoff is produced by the model
 487 during the October event and much less during the November event:

488 a) The first stands in the rainfall intensities. Fig.4c shows that the October
 489 event, shorter, was associated with larger rainfall intensities than the Novem-
 490 ber event. High rainfall intensities strongly increase the probability of the

491 model to produce infiltration excess overland flow. This is what happens dur-
492 ing the simulation of the October event;

493

494 b) The second reason is linked to the location of the rainfall, as regard as the soil
495 properties. The largest part of the precipitation of the November event was
496 located on the mountainous area of the Cevennes-Vivarais region (western part
497 of the catchments). This area is mainly covered by forest, with a steep terrain
498 and permeable soils located on cristalline or metamorphic rocks, whereas the
499 soils encountered in the sedimentary plain area, dominated by agricultural
500 land uses, are found to be much less conductive, as shown by experimental *in*
501 *situ* infiltration measurements (Desprats *et al.*, 2010). This also explains the
502 tendency of the model to mainly simulate surface runoff on the plain areas
503 affected by the October event, and groundwater flow on the areas affected by
504 the November event.

505 Results presented in Fig.7 and Fig.8, despite they provide usefull informa-
506 tion on the spatio-temporal differences between events and on the corresponding
507 simulated streamflow processes, should be considered with caution because they
508 are only model results. In the folowing sections, those results are compared to
509 observations.

510 *4.2.2. Regional evaluation of the simulations*

511 *Small-to-medium scale (1-100 km²) evaluation: comparison to post-flood sur-*
512 *vey estimates*

513

514 Since the October 21 - 23 event caused damages (road cuts, landslides, flooding
515 of several places), a post-flood event survey was thus organized. Peak discharges

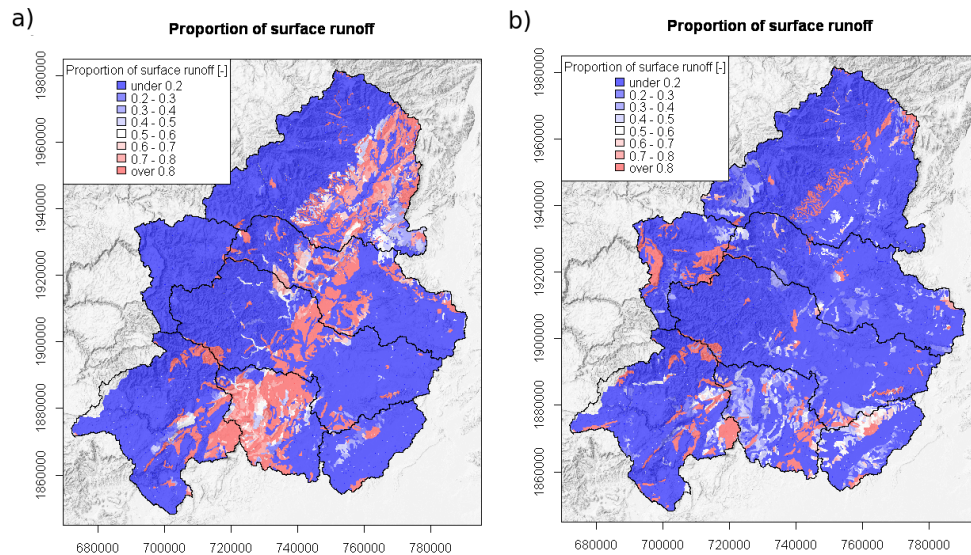


Figure 8: Maps of the ratio between surface runoff and groundwater flow simulated by the CVN-p model. a) October 21 - October 23, 2008 event; (b) October 31 - November 5, 2008 event. The contours of the cumulated kriged rainfall amounts appear in blue.

516 were estimated in 35 locations according to the methodology described by Gaume
517 & Borga (2008). Fig.9 compares simulated specific peak discharges to post-flood
518 survey estimates. We choose to confront specific peak discharge instead of ab-
519 solute peak discharge for an enhanced regional overview of the results. A look
520 at fig.9a) and b) shows that the CVN-p model simulates two areas where specific
521 discharge values are larger than $12 \text{ m}^3 \cdot \text{s}^{-1} \cdot \text{km}^{-2}$: a first one at the border be-
522 tween the Gardon and the Ceze catchments, and a second at the southern border
523 between the Gardon and the Vidourle catchments. These two zones correspond
524 to the two most investigated areas during the post-flood event survey, since they
525 were the most affected by the flood. Globally, the spatial coherence between
526 simulated and estimated discharges is relatively good. Zones where post-flood in-
527 vestigations estimated large values of discharge are also reproduced by the model,
528 and conversely zones where discharge values remained low during the flood event

529 are generally not associated with large values of simulated discharges.

530

531 Nevertheless, there is no perfect correspondence between simulated discharges
532 and post-flood survey estimates. The scatterplot shown in fig.9c) gives a more
533 precise overview of the relationship existing between simulated values and post-
534 flood survey estimates. It shows the existence of a clear linear correlation between
535 estimations and simulated values ($R^2=0.59$), even if the spread around the cen-
536 tral tendency is non negligible. The reasons of these differences stand both in the
537 model and in the post-flood survey methodology uncertainties. Fig.9c) highlights
538 a particular behaviour of the model: the range of variability of the CVN-p results
539 (4 to $19 \text{ m}^3.\text{s}^{-1}.\text{km}^{-2}$) is narrower than the range of variability of the post-flood
540 survey estimates (1 to $26 \text{ m}^3.\text{s}^{-1}.\text{km}^{-2}$). This characteristic is linked to the ten-
541 dency of the model to over-estimate small discharge values and to under-estimate
542 large discharge values. A possible reason for this behaviour would stand in the
543 use of hourly kriged rainfall maps with a spatial resolution of 1 km^2 : such rainfall
544 fields may spatially (as a result of the interpolation process) and temporally (as a
545 result of the measurements hourly timestep) smooth the actual rainfall intensities.

546

547 *Medium-to-large scale (30-2000 km²) evaluation: comparison to streamgauges*
548 *measurements*

549

550 Fig.10 presents an evaluation of the simulations for the two flood events. These
551 maps show the calculated value of the three performance criteria previously intro-
552 duced (NSE, PBIAS and R2), computed at all the gauging sites. On these maps,
553 the size of the circles gives the magnitude of the observed peak discharge, thus
554 indicating the relative importance that must be accorded to the computed score

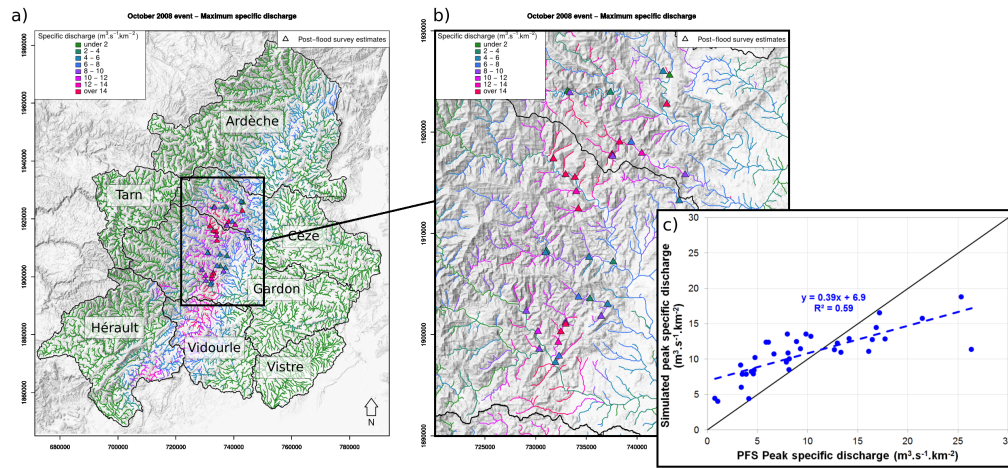


Figure 9: Comparison of the peak specific discharges simulated on each river reach to the peak specific discharge estimated during the post-flood survey, for the October 21 - October 23, 2008 event. River reaches and points denoting the location of the post-flood survey (PFS) estimates are coloured according to the magnitude of the peak specific discharge. a) Map of the regional simulation results; b) Zoom on the locations of post-flood survey estimates; c) Scatter plot of the results.

555 at this location.

556

557 Fig.10 clearly indicates very distinct performances obtained by the model, de-
 558 pending on the considered catchment. On the Ardèche and the Tarn catchments,
 559 the model provides fair results (for a non-calibrated model) in terms of Nash-
 560 Sutcliffe Efficiencies for both events (note that the October event did not affect
 561 strongly the Tarn river), with positive NSE, with a score larger than 0.4 on most
 562 of the gauging locations. By contrast, the results obtained on the other catch-
 563 ments (Cèze, Gardon, Vistre, Vidourle, Hérault) are poor, with negative values
 564 of NSE calculated almost everywhere, for both events.

565

566 The maps of the computed PBIAS and R2 scores provide usefull insights for
 567 the understanding of the reasons of such distinct behaviours. The scores obtained

568 in terms of R2 and PBIAS do not present similar spatial patterns. While the
569 PBIAS scores map is comparable to the NSE scores map, with a clear separation
570 between the good (Tarn and the Ardèche) and the poor (elsewhere) performances
571 obtained, the correlation coefficient R2 does not present a clear spatial pattern.
572 The correlation coefficients calculated for the Tarn and Ardèche catchments do
573 not clearly differ from the values obtained on the other part of the region. This is
574 particularly true for the second event (November), where R2 values are relatively
575 good everywhere, with most of the simulated hydrographs presenting correlations
576 coefficient towards observed hydrographs larger than 0.85. This result indicates
577 the good ability of the CVN-p model to reproduce the flow dynamics of the catch-
578 ments (i.e. the shape and the timing of the observed floods).

579

580 On the other hand, the model does not properly reproduce the observed flood
581 volumes everywhere, as evidenced by the PBIAS score values obtained. For the
582 largest part of the catchments, CVN-p overestimates flood volumes, with com-
583 puted values of PBIAS larger than +40%. Interestingly, for the Tarn and Ardèche
584 catchments, the simulated volumes are much more realistic, with obtained PBIAS
585 scores lower than 20%, and even negative (underestimation of volumes) at several
586 locations. These spatial patterns of the NSE and PBIAS scores suggest that the
587 model generally overestimates flood volumes while the dynamics of the flood is
588 satisfyingly reproduced (as shown by the R2 scores map).

589

590 The most likely interpretation of these results stands in the geological na-
591 ture of the catchments. As shown in Fig.3, the Ardèche and Tarn catchments
592 include large areas of crystalline rocks (granite and gneiss). This type of rocks
593 is even dominant in the northern part of the Tarn catchment, and on the upper

594 (mountainous) part of the Ardèche catchment, where the November 2008 event
595 was the most intense. The results shown in Fig 10 thus confirm and extend those
596 presented in section 4.1. The tendency of the model to perform well on a cer-
597 tain type of geology and not on others is thus confirmed at the regional scale.
598 These results also prove that the performances are not event-dependent: both
599 flood events provide very similar results. We can thus claim that our results only
600 arise from the structure of the hydrological model and from its parametrization,
601 and can consequently be reproduced for other flood events.

602

603 5. Discussion

604 *The role of the sub-soil compartment in the streamflow dynamics*

605

606 The results of section 4.1 suggest the importance of the sub-soil compartment
607 in the long-term dynamics as well as in the flood event response of catchments.
608 Vannier *et al.* (2014) showed the necessity to account for sub-soil (i.e. weathered
609 rock layers) water storage capacity to correctly reproduce the water balance of
610 Cevennes-Vivarais catchments. The direct implementation of a weathered rock
611 layer into the regional rainfall-runoff model CVN-p, with the parametrization
612 proposed by Vannier *et al.* (2014), involves a massive - although unequal - im-
613 provement of the model results, both for flood event and long-term simulations.

614

615 These findings confirm the need to properly represent the overall water storage
616 capacity of catchments into hydrological models (Sayama *et al.*, 2011). Because of
617 a generalized lack of reliable information on the water retention capacity of rocks
618 that compose the sub-soil compartment, hydrologists often rely on calibration of

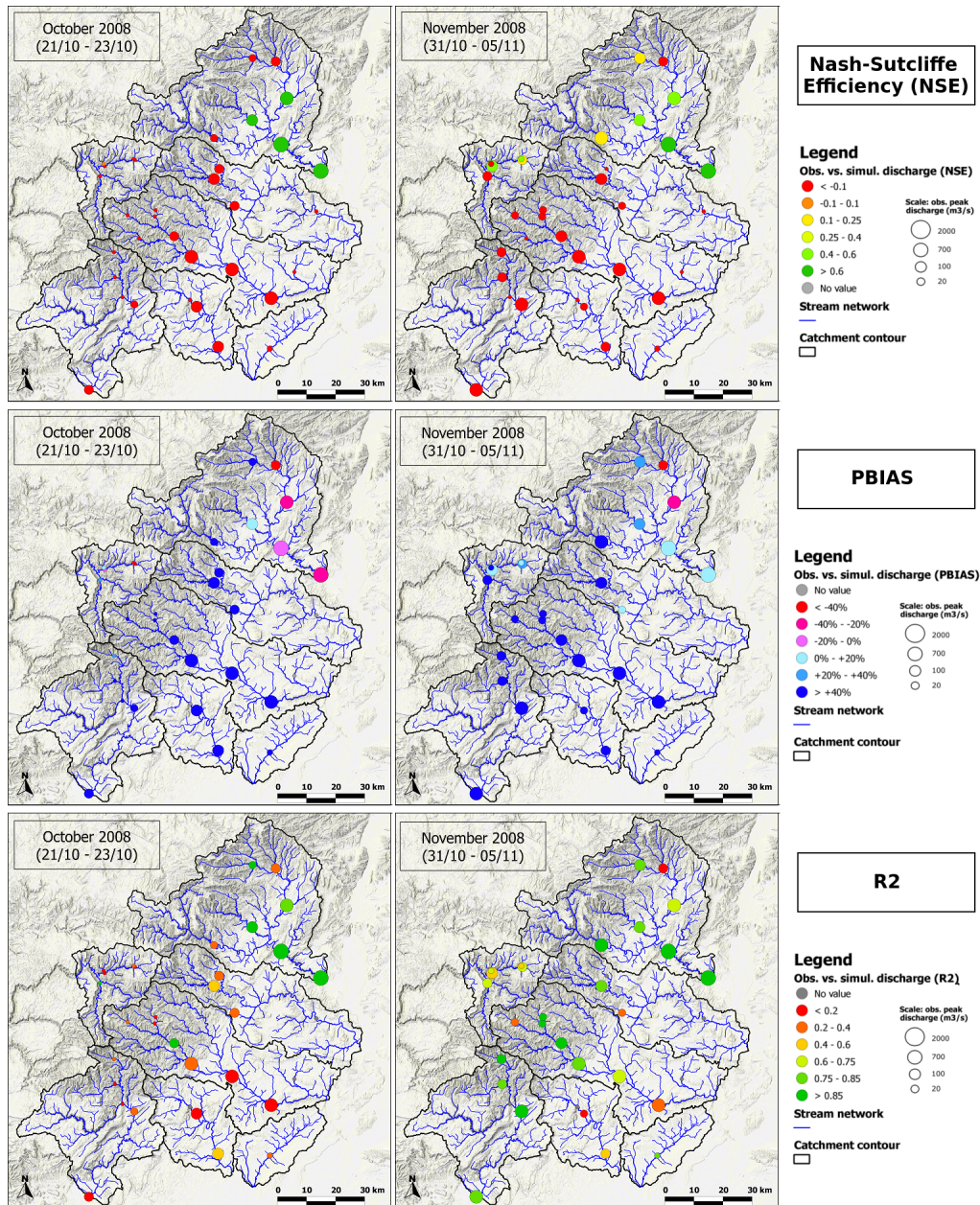


Figure 10: Spatial representation of the performance indices calculated for the simulations of the two flood events of year 2008 in the Cevennes-Vivarais region, using the CVN-p rainfall-runoff model and using the weathered rocks horizons.

619 this parameter. Sometimes, models and their water storage capacities are set up
620 using the knowledge provided by soil databases (Manus *et al.*, 2009; Braud *et al.*,
621 2010, e.g.). Only considering soil horizons can lead to the use of correction coef-
622 ficients to account for an effective water storage capacity, generally much larger
623 than the soil storage capacity (Roux *et al.*, 2011; Garambois *et al.*, 2015). To
624 face the lack of available data which can be used in process-oriented distributed
625 models, the present study demonstrates the applicability and reliability of the
626 method proposed by Vannier *et al.* (2014) to add a weathered rock layer below
627 upper soil horizons and to characterize it in terms of effective thickness and hy-
628 draulic conductivity.

629

630 *The different hydrological behaviours induced by distinct geologies*

631

632 The present work shows that in the Cevennes-Vivarais region, geology appears
633 as an important control factor over the hydrological behaviour of catchments. The
634 response of crystalline catchments is properly reproduced by the model, but the
635 results remain perfectible for schist-dominated catchments. Several sensitivity
636 studies (not shown) have been performed on these schist catchments to see if this
637 could have had a positive impact on the simulated streamflow dynamics. The
638 result is that no different parameters combination turned out to provide better
639 simulation results than those presented in this article. This highlights a lack in
640 the model structure more than in the parametrization. It is important to add
641 that the results shown here are not specific to the two events selected. The gar-
642 don catchment, for which the CVN-p model overestimates both volume and peak
643 discharge during the October 2008 event, behaves similarly during the November
644 2008 event (this is not shown here, but results are presented in Vannier (2013)). In

645 addition, simulations were performed on another flood event that impacted both
646 the Tarn (crystalline rocks) and the upper Gardon (schists): the 19-20 October
647 2006 event. Results, not shown here, are almost identical to those discussed in
648 this study. This proves the robustness of the results presented here.

649

650 If the model structure is not able to reproduce the storage and draining be-
651 haviour of weathered schist rock layers, whatever the thickness and conductivity
652 considered, this means that this geology acts differently than crystalline rocks
653 on the sub-surface flowpaths and thus on the response of the catchments. The
654 potential hydrologic specificity of schist rocks, despite poorly described in litter-
655 ature, has been suggested by Martin *et al.* (2004) and Maréchal *et al.* (2013),
656 both looking at french mediterranean catchments. In these two studies, the au-
657 thors observe that schist catchments behave differently from others. Martin *et al.*
658 (2004) assume that the planar structure of schisty rocks represents a preferential
659 sloping direction for the subsurface or groundwater flows and that consequently,
660 depending on the direction of the schist layers regarding the topography, schists
661 can whether accelerate groundwater flows or increase water storage. We believe
662 that this behaviour largely explains the results presented here. Of course, this
663 assumption needs to be confirmed, through other modelling studies as well as
664 complementary observations.

665

666 *Usefulness of process-oriented and multi-scale regional models*

667

668 Through this work, we hope to convince hydrologists about the usefulness
669 of regional process-oriented models. Three important features of the modelling
670 approach used here are highlighted:

671 1. *A regional set-up of the model.* As opposed to most of the modelling works
672 performed in the Cevennes-Vivarais region, focusing on a single catchment,
673 the present study covers the entire region (seven catchments, with an area of
674 several thousands of km²). This regional approach allows a direct comparison
675 of the simulated streamflow dynamics of catchments which can differ by their
676 physiographic characteristics (such as geology). This inter-catchments compar-
677 ison, coupled to a classical evaluation of the goodness of the simulations, re-
678 veals some important behavioural differences existing between catchments that
679 would have been difficult to detect using a classical catchment-by-catchment
680 modelling approach.

681

682 2. *A multiscale modelling strategy.* Another important characteristic of the mod-
683 elling strategy followed here stands in the wide range of spatial scales covered
684 by CVN-p. The continuity between scales, from the elementary response unit
685 (< 1 km²) to the outlet of the largest catchments (> 2000 km²), gives an
686 integrated view of the hydrological response to flood events. It allows a mean-
687 ingfull multiscale comparison of different flood events and of their magnitude,
688 such as in Fig.7.

689

690 3. *An uncalibrated modelling approach.* The absence of calibration is not an end
691 in itself, but is necessary in the purpose of testing hydrological functioning
692 hypotheses. The strength of this approach is illustrated in this study when
693 assessing the contribution of the weathered rock layers in the model perfor-
694 mance: the parameters that characterize the weathered rock horizons are not
695 calibrated, the values estimated by Vannier *et al.* (2014) are directly given
696 as input into the model. Through this approach, we found out the adequate

697 model structure to reproduce the dynamics of crystalline rock catchments and
698 discovered that this structure is not suitable for schist rocks catchments.
699

700 6. Conclusions

701 This work represents a step towards a better understanding of the govern-
702 ing hydrological processes in the mediterranean area, and especially on the role
703 played by geology in catchments prone to flash floods. Through a regional mul-
704 tiscale hydrological modelling approach, focusing both on event and inter-event
705 (long term) simulations, we assess the effect of adding weathered rock layers into
706 the model, with hydraulic properties varying with geology and estimated after
707 the results obtained by Vannier *et al.* (2014). Simulation results highlight the
708 importance of the sub-soil layers and their associated storage capacity in the gen-
709 eral streamflow dynamic of catchments, during and between flood events. Results
710 also enhance some behavioural differences between catchments, related to their
711 dominant geology. The addition of sub-soil layers in the CVN-p model largely im-
712 proves the results, and allows to satisfyingly reproduce the streamflow dynamic
713 and the flood response of crystalline rocks catchments. On other geologies, the
714 improvement is real but still not sufficient to perfectly agree with the observations.
715

716 On a methodological point of view, this work proves the reliability of uncal-
717 ibrated, process-oriented modelling studies, especially when set up at a regional
718 scale. Such approaches are very effective to bring out behavioural similarities or
719 differences between neighbouring catchments, or to identify the key hydrologi-
720 cal processes over a wide range of spatial and temporal scales. Combined with
721 a multi-criteria evaluation strategy, and proceeding in an iterative way to test

722 hydrological functioning hypotheses, such modeling approaches need to be en-
723 couraged and developed.

724

725 Further field observations and modelling studies are required to confirm the
726 preliminary results obtained and shown in this work, especially to investigate and
727 better reproduce the groundwater transfers that exist in schists and sedimentary
728 rocks sub-soil layers. We also recommend to use similar modelling approaches over
729 different regions and under other climatic conditions, to assess the robustness of
730 the proposed methodology.

731

732 **7. Acknowledgements**

733 This work is part of the FloodScale project, which is funded by the French
734 National Research Agency (ANR) under contract n° ANR 2011 BS56 027, which
735 contributes to the HyMeX program. The authors would like to acknowledge
736 Jérémy Chardon, from LTHE, for supplying the 10-years return period quantiles
737 of SAFRAN daily rainfall depths.

738 **References**

- 739 ALFIERI, L., SMITH, P. J., Thielen-del POZO, J. & BEVEN, K. J. : A staggered approach to flash
740 flood forecasting – case study in the Cévennes region. *Advances in Geosciences*, 29:13–20,
741 2011.
- 742 ALLEN, R. G., PEREIRA, L. S., RAES, D. & SMITH, M. : *Crop evapotranspiration - Guidelines*
743 *for computing crop water requirements*, volume 56. Food and Agriculture Organization of the
744 United Nations (F.A.O.), 1998.

- 745 ANQUETIN, S., BRAUD, I., VANNIER, O., VIALLET, P., BOUDEVILLAIN, B., CREUTIN, J.-D. &
746 MANUS, C. : Sensitivity of the hydrological response to the variability of rainfall fields and
747 soils for the Gard 2002 flash-flood event. *Journal of Hydrology*, 394(1-2):134–147, 2010.
- 748 AUBERT, Y., ARNAUD, P., RIBSTEIN, P. & FINE, J.-A. : The SHYREG flow method—application
749 to 1605 basins in metropolitan France. *Hydrological Sciences Journal*, 59(5):993–1005, 2014.
- 750 BLUME, T., ZEHE, E., REUSSER, D. E., IROUMÉ, A. & BRONSTERT, A. : Investigation of runoff
751 generation in a pristine, poorly gauged catchment in the Chilean Andes I: A multi-method
752 experimental study. *Hydrological Processes*, 22(18):3661–3675, 2008.
- 753 BONNIFAIT, L., DELRIEU, G., LE LAY, M., BOUDEVILLAIN, B., MASSON, A., BELLEUDY, P.,
754 GAUME, E. & SAULNIER, G.-M. : Distributed hydrologic and hydraulic modelling with radar
755 rainfall input: Reconstruction of the 8-9 September 2002 catastrophic flood event in the Gard
756 region, France. *Advances in Water Resources*, 32(7):1077–1089, 2009.
- 757 BOUDEVILLAIN, B., DELRIEU, G., GALABERTIER, B., BONNIFAIT, L., BOUILLOU, L., KIRSTET-
758 TER, P.-E. & MOSINI, M.-L. : The Cévennes-Vivarais mediterranean hydrometeorological ob-
759 servatory database. *Water Resources Research*, 47(7):W07701, doi:10.1029/2010WR010353,
760 2011.
- 761 BOUILLOU, L., CHANCIBAULT, K., VINCENDON, B., DUCROCQ, V., HABETS, F., SAULNIER, G.-
762 M., ANQUETIN, S., MARTIN, E. & NOILHAN, J. : Coupling the ISBA land surface model and
763 the TOPMODEL hydrological model for mediterranean flash-flood forecasting: Description,
764 calibration, and validation. *Journal of Hydrometeorology*, 11(2):315–333, 2010.
- 765 BRANGER, F., BRAUD, I., DEBIONNE, S., VIALLET, P., DEHOTIN, J., HENINE, H., NEDELEC, Y.
766 & ANQUETIN, S. : Towards multi-scale integrated hydrological models using the LIQUID®
767 framework. Overview of the concepts and first application examples. *Environmental Modelling*
768 *& Software*, 25(12):1672–1681, 2010.
- 769 BRAUD, I., AYRAL, P.-A., BOUVIER, C., BRANGER, F., DELRIEU, G., LE COZ, J., NORD, G.,
770 VANDERVAERE, J.-P., ANQUETIN, S., ADAMOVIC, M., ANDRIEU, J., BATIOU, C., BOUDEVIL-
771 LAIN, B., BRUNET, P., CARREAU, J., CONFOLAND, A., DIDON-LESCOT, J.-F., DOMERGUE,
772 J.-M., DOUVINET, J., DRAMAIS, G., FREYDIER, R., GÉRARD, S., HUZA, J., LEBLOIS, E.,
773 LE BOURGEOIS, O., LE BOURSICAUD, R., MARCHAND, P., MARTIN, P., NOTTALE, L., PATRIS,
774 N., RENARD, B., SEIDEL, J.-L., TAUPIN, J.-D., VANNIER, O., VINCENDON, B. & WIJBRANS,
775 A. : Multi-scale hydrometeorological observation and modelling for flash flood understanding.

- 776 *Hydrology and Earth System Sciences*, 18(9):3733–3761, 2014.
- 777 BRAUD, I., ROUX, H., ANQUETIN, S., MAUBOURGUET, M.-M., MANUS, C., VIALLET, P. &
778 DARTUS, D. : The use of distributed hydrological models for the Gard 2002 flash flood event:
779 Analysis of associated hydrological processes. *Journal of Hydrology*, 394(1-2):162–181, 2010.
- 780 BROOKS, R. H. & COREY, A. T. : Hydraulic properties of porous media. *Hydrology Papers*,
781 *Colorado State University*, 1964.
- 782 BRUTSAERT, W. & NIEBER, J. L. : Regionalized drought flow hydrographs from a mature
783 glaciated plateau. *Water Resources Research*, 13(3):637–643, 1977.
- 784 CASERI, A., JAVELLE, P., RAMOS, M. & LEBLOIS, E. : Generating precipitation ensembles for
785 flood alert and risk management. *Journal of Flood Risk Management*, 2015.
- 786 CERESSETTI, D. : *Structure spatio-temporelle des fortes précipitations : application à la région*
787 *Cévennes-Vivarais*. Thèse de doctorat, Université de Grenoble, 2011.
- 788 CLARK, M. P., KAVETSKI, D. & FENICIA, F. : Pursuing the method of multiple work-
789 ing hypotheses for hydrological modeling. *Water Resources Research*, 47(9):W09301,
790 doi:10.1029/2010WR009827, 2011.
- 791 CREVOISIER, D., CHANZY, A. & VOLTZ, M. : Evaluation of the Ross fast solution of Richards'
792 equation in unfavourable conditions for standard finite element methods. *Advances in Water*
793 *Resources*, 32(6):936–947, 2009.
- 794 CRUPEDIX : (la méthode). Fascicule 3 de la Synthèse nationale sur les crues des petits bassins
795 versants (in french). Rapport technique, French Ministry of Agriculture., July 1980.
- 796 DE MICHELE, C., KOTTEGODA, N. T. & ROSSO, R. : The derivation of areal reduction factor
797 of storm rainfall from its scaling properties. *Water Resources Research*, 37(12):3247–3252,
798 2001.
- 799 DEHOTIN, J. & BRAUD, I. : Which spatial discretization for distributed hydrological mod-
800 els? Proposition of a methodology and illustration for medium to large-scale catchments.
801 *Hydrology and Earth System Sciences*, 12(3):769–796, 2008.
- 802 DESPRATS, J.-F., CERDAN, O., KING, C. & MARCHANDISE, A. : Cartographie de la perméabilité
803 des sols pour l'aide à la prévision des crues; cas d'étude sur le Gardon d'Anduze. *La Houille*
804 *Blanche*, 3:32–38, 2010.
- 805 FENICIA, F., KAVETSKI, D. & SAVENIJE, H. H. G. : Elements of a flexible approach for conceptual
806 hydrological modeling: 1. Motivation and theoretical development. *Water Resources Research*,

- 807 47(11):W11510, doi: 10.1029/2010WR010174, 2011.
- 808 FENICIA, F., MCDONNELL, J. J. & SAVENIJE, H. H. G. : Learning from model improvement: On
809 the contribution of complementary data to process understanding. *Water Resources Research*,
810 44(6):W06419, doi:10.1029/WR006386, 2008a.
- 811 FENICIA, F., SAVENIJE, H. H. G., MATGEN, P. & PFISTER, L. : Understanding catchment
812 behavior through stepwise model concept improvement. *Water Resources Research*, 44(1):
813 n/a–n/a, 2008b.
- 814 GARAMBOIS, P.-A., ROUX, H., LARNIER, K., CASTAINGS, W. & DARTUS, D. : Characterization
815 of process-oriented hydrologic model behavior with temporal sensitivity analysis for flash
816 floods in Mediterranean catchments. *Hydrology and Earth System Sciences*, 17(6):2305–2322,
817 2013.
- 818 GARAMBOIS, P., ROUX, H., LARNIER, K., LABAT, D. & DARTUS, D. : Characterization of
819 catchment behaviour and rainfall selection for flash flood hydrological model calibration:
820 catchments of the eastern Pyrenees. *Hydrological Sciences Journal*, 60(3):424–447, 2015.
- 821 GAUME, E., BAIN, V., BERNARDARA, P., NEWINGER, O., BARBUC, M., BATEMAN, A.,
822 BLASKOVICOVÁ, L., BLÖSCHL, G., BORGA, M., DUMITRESCU, A., DALIAKOPOULOS, I., GAR-
823 CIA, J., IRIMESCU, A., KOHNOVA, S., KOUTROULIS, A., MARCHI, L., MATREATA, S., MEDINA,
824 V., PRECISO, E., SEMPERE-TORRES, D., STANCALIE, G., SZOLGAY, J., TSANIS, I., VELASCO,
825 D. & VIGLIONE, A. : A compilation of data on European flash floods. *Journal of Hydrology*,
826 367(1-2):70 – 78, 2009.
- 827 GAUME, E. & BORGA, M. : Post-flood field investigations in upland catchments after major
828 flash floods: proposal of a methodology and illustrations. *Journal of Flood Risk Management*,
829 1(4):175–189, 2008.
- 830 GHARARI, S., HRACHOWITZ, M., FENICIA, F., GAO, H. & SAVENIJE, H. H. G. : Using expert
831 knowledge to increase realism in environmental system models can dramatically reduce the
832 need for calibration. *Hydrology and Earth System Sciences*, 18(12):4839–4859, 2014.
- 833 HRACHOWITZ, M., SAVENIJE, H. H. G., BLÖSCHL, G., MCDONNELL, J. J., SIVAPALAN, M.,
834 POMEROY, J. W., ARHEIMER, B., BLUME, T., CLARK, M. P., EHRET, U., FENICIA, F.,
835 FREER, J. E., GELFAN, A., GUPTA, H. V., HUGHES, D. A., HUT, R. W., MONTANARI, A.,
836 PANDE, S., TETZLAFF, D., TROCH, P. A., UHLENBROOK, S., WAGENER, T., WINSEMIUS,
837 H. C., WOODS, R. A., ZEHE, E. & CUDENNEC, C. : A decade of Predictions in Ungauged

- 838 Basins (PUB) - a review. *Hydrological Sciences Journal*, 58(6):1–58, 2013.
- 839 HUYGEN, J., VAN DAM, J. C., KROES, J. G. & WESSELING, J. G. : SWAP 2.0: input and
840 output manual. Rapport technique, Wageningen Agricultural University, and DLO-Staring
841 Centrum, Wageningen., 1997.
- 842 JAVELLE, P., DEMARGNE, J., DEFRANCE, D., PANSU, J. & ARNAUD, P. : Evaluating flash-
843 flood warnings at ungauged locations using post-event surveys: a case study with the AIGA
844 warning system. *Hydrological Sciences Journal*, 59(7):1390–1402, 2014.
- 845 KANG, B. & TRIPATHI, B. : *The AFNETA alley farming training manual - Volume 2: Source*
846 *book for alley farming research*, chapitre Technical paper 1 : soil classification and character-
847 ization. Food and Agriculture Organization of the United Nations (F.A.O.), 1992.
- 848 KAVETSKI, D. & FENICIA, F. : Elements of a flexible approach for conceptual hydrological
849 modeling: 2. Application and experimental insights. *Water Resources Research*, 47:W11511,
850 doi: 10.1029/2011WR01748, 2011.
- 851 KLING, H. & GUPTA, H. : On the development of regionalization relationships for lumped
852 watershed models: The impact of ignoring sub-basin scale variability. *Journal of Hydrology*,
853 373(3-4):337 – 351, 2009.
- 854 LATRON, J. & GALLART, F. : Runoff generation processes in a small Mediterranean research
855 catchment (Vallcebre, Eastern Pyrenees). *Journal of Hydrology*, 358(3-4):206–220, 2008.
- 856 LE LAY, M. & SAULNIER, G.-M. : Exploring the signature of climate and landscape spatial vari-
857 abilities in flash flood events: Case of the 8-9 September 2002 Cévennes-Vivarais catastrophic
858 event. *Geophysical Research Letters*, 34(13):L13401, doi:10.1029/2007GL029746, 2007.
- 859 LI, K. Y., DE JONG, R. & BOISVERT, J. B. : An exponential root-water-uptake model with
860 water stress compensation. *Journal of Hydrology*, 252(1-4):189–204, 2001.
- 861 MANUS, C., ANQUETIN, S., BRAUD, I., VANDERVAERE, J.-P., CREUTIN, J.-D., VIALLET, P. &
862 GAUME, E. : A modeling approach to assess the hydrological response of small mediterranean
863 catchments to the variability of soil characteristics in a context of extreme events. *Hydrology*
864 *and Earth System Sciences*, 13(2):79–97, 2009.
- 865 MARÉCHAL, D., AYRAL, P.-A., BAILLY, J.-S., PUECH, C. & SAUVAGNARGUES-LESAGE, S. :
866 Sur l'origine morphologique des écoulements par l'analyse d'observations hydrologiques dis-
867 tribuées. Application à deux bassins versants cévenols (Gard, France). *Géomorphologie :
868 relief, processus, environnement*, 1:47–62, 2013.

- 869 MARTIN, F., MARTIN, C., LAVABRE, J. & FOLTON, N. : Fonctionnement hydrologique des
870 bassins versants de roches métamorphiques : exemple du bassin versant des Maurets (massif
871 des Maures, Var, France). *Études de Géographie Physique*, 31:39–70, 2004.
- 872 MASSON, V., CHAMPEAUX, J.-L., CHAUVIN, F., MERIGUET, C. & LACAZE, R. : A global
873 database of land surface parameters at 1-km resolution in meteorological and climate models.
874 *Journal of Climate*, 16(9):1261–1282, 2003.
- 875 McMILLAN, H., FREER, J., PAPPENBERGER, F., KRUEGER, T. & CLARK, M. : Impacts of
876 uncertain river flow data on rainfall-runoff model calibration and discharge predictions. *Hy-*
877 *drological Processes*, 24(10):1270–1284, 2010.
- 878 McNAMARA, J. P., TETZLAFF, D., BISHOP, K., SOULSBY, C., SEYFRIED, M., PETERS, N. E.,
879 AULENBACH, B. T. & HOOPER, R. : Storage as a Metric of Catchment Comparison. *Hydro-*
880 *logical Processes*, 25(21):3364–3371, 2011.
- 881 MONTEITH, J. L. : Evaporation and environment. In: The State and Movement of Water in
882 Living Organisms. *In the XIXth Symposia of the Society for Experimental Biology (Swansea,*
883 *UK)*, pages 205–234, 1965.
- 884 NASH, J. E. & SUTCLIFFE, J. V. : River flow forecasting through conceptual models part I - A
885 discussion of principles. *Journal of Hydrology*, 10(3):282–290, 1970.
- 886 NESTER, T., KIRNBAUER, R., GUTKNECHT, D. & BLÖSCHL, G. : Climate and catchment controls
887 on the performance of regional flood simulations. *Journal of Hydrology*, 402(3-4):340–356,
888 2011.
- 889 NOILHAN, J. & PLANTON, S. : A simple parameterization of land surface processes for meteo-
890 rological models. *Monthly Weather Review*, 117(3):536–549, 1989.
- 891 NOTO, L., IVANOV, V., BRAS, R. & VIVONI, E. : Effects of initialization on response of a
892 fully-distributed hydrologic model. *Journal of Hydrology*, 352(1-2):107 – 125, 2008.
- 893 OUDIN, L., ANDRÉASSIAN, V., PERRIN, C., MICHEL, C. & LE MOINE, N. : Spatial proxim-
894 ity, physical similarity, regression and ungaged catchments: A comparison of regionaliza-
895 tion approaches based on 913 French catchments. *Water Resources Research*, 44(3):W03413,
896 doi:10.1029/2007WR006240, 2008.
- 897 OUDIN, L., KAY, A., ANDRÉASSIAN, V. & PERRIN, C. : Are seemingly physically similar
898 catchments truly hydrologically similar? *Water Resources Research*, 46(11):n/a–n/a, 2010.
- 899 PARAJKA, J., MERZ, R. & BLÖSCHL, G. : A comparison of regionalisation methods for catchment

- 900 model parameters. *Hydrology and Earth System Sciences*, 9(3):157–171, 2005.
- 901 PARAJKA, J., VIGLIONE, A., ROGGER, M., SALINAS, J. L., SIVAPALAN, M. & BLÖSCHL, G.
902 : Comparative assessment of predictions in ungauged basins - Part 1: Runoff-hydrograph
903 studies. *Hydrology and Earth System Sciences*, 17(5):1783–1795, 2013.
- 904 QUINTANA-SEGUÍ, P., LE MOIGNE, P., DURAND, Y., MARTIN, E., HABETS, F., BAILLON, M.,
905 CANELLAS, C., FRANCHISTEGUY, L. & MOREL, S. : Analysis of near-surface atmospheric
906 variables: Validation of the SAFRAN analysis over France. *Journal of Applied Meteorology*
907 *and Climatology*, 47(1):92–107, 2008.
- 908 RAWLS, W. J. & BRAKENSIEK, D. L. : Prediction of soil water properties for hydrologic modeling.
909 *In Watershed Management in the Eighties*, pages 293–299. Proceedings of a Symposium ASCE
910 (Denver, USA), 1985.
- 911 REGGIANI, P., HASSANIZADEH, S. M., SIVAPALAN, M. & GRAY, W. G. : A unifying framework
912 for watershed thermodynamics: constitutive relationships. *Advances in Water Resources*, 23
913 (1):15–39, 1999.
- 914 REGGIANI, P., SIVAPALAN, M. & HASSANIZADEH, S. M. : A unifying framework for watershed
915 thermodynamics: balance equations for mass, momentum, energy and entropy, and the second
916 law of thermodynamics. *Advances in Water Resources*, 22(4):367–398, 1998.
- 917 RICHARDS, L. A. : Capillary conduction of liquids through porous mediums. *Journal of Applied*
918 *Physics*, 1(5):318–333, 1931.
- 919 RINALDO, A., BEVEN, K., BERTUZZO, E., NICOTINA, L., DAVIES, J., FIORI, A., RUSSO, D. &
920 BOTTER, G. : Catchment travel time distributions and water flow in soils. *Water Resources*
921 *Research*, 47, JUL 20 2011.
- 922 ROBBEZ-MASSON, J. M., BARTHES, J. P., BORNAND, M., FALIPOU, P. & LEGROS, J. P. : Bases
923 de données pédologiques et systèmes d'informations géographiques. L'exemple de la région
924 Languedoc-Roussillon. *Forêt Méditerranéenne*, 21(1):88–98, 2000.
- 925 ROSS, P. J. : Modeling soil water and solute transport - Fast, simplified numerical solutions.
926 *Agronomy Journal*, 95(6):1352–1361, 2003.
- 927 ROUX, H., LABAT, D., GARAMBOIS, P.-A., MAUBOURGUET, M.-M., CHORDA, J. & DARTUS,
928 D. : A physically-based parsimonious hydrological model for flash floods in Mediterranean
929 catchments. *Natural Hazards and Earth System Science*, 11(9):2567–2582, 2011.
- 930 SALINAS, J., LAAHA, G., ROGGER, M., PARAJKA, J., VIGLIONE, A., SIVAPALAN, M. & BLÖSCHL,

- 931 G. : Comparative assessment of predictions in ungauged basins - Part 2: Flood and low flow
932 studies. *Hydrology and Earth System Sciences*, 17(7):2637–2652, 2013.
- 933 SAVENIJE, H. H. G. : HESS Opinions "Topography driven conceptual modelling (FLEX-Topo)".
934 *Hydrology and Earth System Sciences*, 14(12):2681–2692, 2010.
- 935 SAWICZ, K., WAGENER, T., SIVAPALAN, M., TROCH, P. A. & CARRILLO, G. : Catchment
936 classification: empirical analysis of hydrologic similarity based on catchment function in the
937 eastern USA. *Hydrology and Earth System Sciences*, 15(9):2895–2911, 2011.
- 938 SAYAMA, T., McDONNELL, J. J., DHAKAL, A. & SULLIVAN, K. : How much water can a
939 watershed store? *Hydrological Processes*, 25(25):3899–3908, 2011.
- 940 SAYAMA, T. & McDONNELL, J. : A new time-space accounting scheme to predict stream water
941 residence time and hydrograph source components at the watershed scale. *Water Resources*
942 *Research*, 45, JUL 1 2009.
- 943 SELKER, J., van de GIESEN, N., WESTHOFF, M., LUXEMBURG, W. & PARLANGE, M. B. : Fiber
944 optics opens window on stream dynamics. *Geophysical Research Letters*, 33(24):n/a–n/a,
945 2006. L24401.
- 946 SIMUNEK, J., SEJNA, M. & van GENUCHTEN, M. T. : *Agronomy Abstracts*, chapitre The
947 HYDRUS-1D and HYDRUS-2D codes for estimating unsaturated soil hydraulic and solutes
948 transport parameters. American Society of Agronomy, 1999.
- 949 SIVAPALAN, M., TAKEUCHI, K., FRANKS, S. W., GUPTA, V. K., KARAMBIRI, H., LAKSHMI, V.,
950 LIANG, X., McDONNELL, J. J., MENDIONDO, E. M., O'CONNELL, P. E., OKI, T., POMEROY,
951 J. W., SCHERTZER, D., UHLENBROOK, S. & ZEHE, E. : IAHS Decade on Predictions in
952 Ungauged Basins (PUB), 2003-2012: Shaping an exciting future for the hydrological sciences.
953 *Hydrological Sciences Journal*, 48(6):857–880, 2003.
- 954 TARBOTON, D. G. : A new method for the determination of flow directions and upslope areas
955 in grid digital elevation models. *Water Resources Research*, 33(2):309–319, 1997.
- 956 TETZLAFF, D., SOULSBY, C., WALDRON, S., MALCOLM, I., BACON, P., DUNN, S., LILLY, A.
957 & YOUNGSON, A. : Conceptualization of runoff processes using a geographical information
958 system and tracers in a nested mesoscale catchment. *Hydrological Processes*, 21(10):1289–
959 1307, 2007.
- 960 TETZLAFF, D., McNAMARA, J. P. & CAREY, S. K. : Measurements and modelling of storage
961 dynamics across scales. *Hydrological Processes*, 25(25):3831–3835, 2011.

- 962 TROCH, P. A., PANICONI, C. & van LOON, E. E. : Hillslope-storage Boussinesq model for subsur-
963 face flow and variable source areas along complex hillslopes: 1. Formulation and characteristic
964 response. *Water Resources Research*, 39(11):1316, doi:10.1029/2002WR001728, 2003.
- 965 Tromp-van MEERVELD, H. J., PETERS, N. E. & MCDONNELL, J. J. : Effect of bedrock perme-
966 ability on subsurface stormflow and the water balance of a trenched hillslope at the Panola
967 Mountain Research Watershed, Georgia, USA. *Hydrological Processes*, 21(6):750–769, 2007.
- 968 VANNIER, O. : *Regional modeling of mediterranean floods : contribution to the understanding*
969 *of the dominant hydrological processes. PhD thesis (in french. Thèse de doctorat, Université*
970 *de Grenoble, 2013.*
- 971 VANNIER, O., BRAUD, I. & ANQUETIN, S. : Regional estimation of catchment-scale soil prop-
972 erties by means of streamflow recession analysis for use in distributed hydrological models.
973 *Hydrological Processes*, 28(26):6276–6291, 2014.
- 974 VARADO, N., BRAUD, I. & ROSS, P. J. : Development and assessment of an efficient vadose zone
975 module solving the 1D Richards' equation and including root extraction by plants. *Journal*
976 *of Hydrology*, 323(1-4):258–275, 2006a.
- 977 VARADO, N., BRAUD, I., ROSS, P. J. & HAVERKAMP, R. : Assessment of an efficient numerical
978 solution of the 1D Richards' equation on bare soil. *Journal of Hydrology*, 323(1-4):244–257,
979 2006b.
- 980 VERSINI, P.-A., GAUME, E. & ANDRIEU, H. : Application of a distributed hydrological model to
981 the design of a road inundation warning system for flash flood prone areas. *Natural Hazards*
982 *and Earth System Science*, 10(4):805–817, 2010.
- 983 VIALLET, P., DEBIONNE, S., BRAUD, I., DEHOTIN, J., HAVERKAMP, R., SAADI, Z., ANQUETIN,
984 S., BRANGER, F. & VARADO, N. : Towards multi-scale integrated hydrological models using
985 the LIQUID framework. *In 7th International Conference on Hydroinformatics. Nice, France,*
986 *pages 542–549, 2006.*
- 987 VIDAL, J.-P., MARTIN, E., FRANCHISTÉGUY, L., BAILLON, M. & SOUBEYROUX, J.-M. : A 50-
988 year high-resolution atmospheric reanalysis over France with the Safran system. *International*
989 *Journal of Climatology*, 30(11):1627–1644, 2010.
- 990 VILLHOLTH, K. & JENSEN, K. H. : Field investigations of preferential flow behaviour. *In Hy-*
991 *drological Interactions Between Atmosphere, Soil and Vegetation (Proceedings of the Vienna*
992 *Symposium).*, 1991.

- 993 VINCENDON, B., DUCROCQ, V., SAULNIER, G.-M., BOUILLOUD, L., CHANCIBAULT, K., HABETS,
994 F. & NOILHAN, J. : Benefit of coupling the ISBA land surface model with a TOPMODEL
995 hydrological model version dedicated to Mediterranean flash-floods. *Journal of Hydrology*,
996 394(1-2):256–266, 2010.
- 997 VIVONI, E., ENTEKHABI, D., BRAS, R. & IVANOV, V. : Controls on runoff generation and
998 scale-dependence in a distributed hydrologic model. *Hydrology and Earth System Sciences*,
999 11(5):1683–1701, 2007.
- 1000 WEILER, M. & McDONNELL, J. J. : Conceptualizing lateral preferential flow and flow networks
1001 and simulating the effects on gauged and ungauged hillslopes. *Water Resources Research*, 43
1002 (3):W03403, doi:10.1029/2006WR004867, 2007.
- 1003 WEILER, M. & NAEF, F. : Simulating surface and subsurface initiation of macropore flow.
1004 *Journal of Hydrology*, 273(1-4):139–154, 2003.
- 1005 YADAV, M., WAGENER, T. & GUPTA, H. V. : Regionalization of constraints on expected
1006 watershed response behavior for improved predictions in ungauged basins. *Advances in Water*
1007 *Resources*, 30(8):1756–1774, 2007.
- 1008 ZEHE, E., GRAEFF, T., MORGNER, M., BAUER, A. & BRONSTERT, A. : Plot and field scale soil
1009 moisture dynamics and subsurface wetness control on runoff generation in a headwater in the
1010 Ore Mountains. *Hydrology and Earth System Sciences*, 14(6):873–889, 2010.

1011 **Appendix A Details on the CVN-p model structure**

1012 A short description of the different hydrological modules coupled within the
1013 continuous CVN-p model, which derives from CVN (Manus *et al.*, 2009) is pre-
1014 sented as follows:

1015

1016 1. Vertical water transfer through soils : FRER1D. The FRER1D module is able
1017 to generate infiltration-excess runoff, as well as saturation excess runoff, even
1018 the one caused by perched water tables (non complete saturation of the soil
1019 profile), since different soil horizons (with different hydraulic properties) can be
1020 described in the model. Relationships between hydraulic conductivity, water
1021 content and soil pressure are provided by the Brooks & Corey (1964) model.
1022 The FRER1D module is an implementation in the LIQUID platform of the
1023 non-iterative Richards' equation (Richards, 1931) solution proposed by Ross
1024 (2003). The Ross methodology to compute one-dimensionnal water transfer in
1025 soils was assessed by Varado *et al.* (2006b). A new version of the numerical
1026 method, accounting for root extraction process by means of the introduction of
1027 sink terms in the Richards' equation, was developped and assessed by Varado
1028 *et al.* (2006a). Crevoisier *et al.* (2009) highlighted the stability and robustness
1029 of the Ross (2003) solution, and showed its superiority towards traditional it-
1030 erative resolution methods, such as those used in commercial tools (Simunek
1031 *et al.*, 1999). Even if the Richards equation resolution in hydrological model
1032 is often presented as a “physically-based” description of water transfer in soils,
1033 we believe this is a common misconception. Many works have shown that the
1034 validity of the Richards equations to describe flow motion is most of the time
1035 restricted to laboratory conditions, with homogeneous porous material subject

1036 to a gradient of charge. In natural conditions, various poorly known processes,
1037 such as rock fracturing or macroporosity, make the actual flow conditions sig-
1038 nificantly differ from Richards theory (Villholth & Jensen, 1991). Therefore,
1039 the use of Richards equations solver in hydrological models, like the FRER1D
1040 module, should rather be considered as a conceptual representation of the ac-
1041 tual processes than as a “physically-based” resolution system.

1042

1043 2. Extraction of ponding and runoff generation: PEM. This module takes as
1044 input the ponding depth (runoff) produced by FRER1D, and sends it - in-
1045 stantaneously - to the closest river reach. Since the river network is finely
1046 described, this instantaneous transfer of runoff into the river does not imply
1047 an unrealistic reduction of the total water transfer time through the catch-
1048 ment. The spatial discretization is based on elementary watersheds with area
1049 that does not exceed 0.5 km². Considering a runoff velocity of 1 m/s before it
1050 reaches the river network, this hypothesis always leads to neglect less than 30
1051 minutes of water transfer time.

1052

1053 3. Water transfer in the river network : RIVER1D. RIVER1D module computes
1054 the routing of water along the river network. It is based on the solution of the
1055 one-dimensionnal kinematic wave equation (Branger *et al.*, 2010).

1056

1057 4. Vegetation and evapotranspiration modules : ROLI, VEGINT, CRLINPG,
1058 ETPART. This set of modules compute the interception and water uptake
1059 from vegetation. Note that despite the addition of the modules, CVN-p is not
1060 a fully coupled water-vegetation model, in the sense that it does neither solve
1061 the vegetation growth nor the energy balance of the system. A reference evap-

1062 otranspiration (ET_0) is used as a forcing, and modulated by crop coefficients,
1063 depending on the vegetation (CRLINPG module). The growth of plants is
1064 prescribed by means of a dynamic evolution of the Leaf Area Index (LAI), as
1065 monthly average values (CRLINPG). VEGINT computes the fraction of water
1066 intercepted by plants during rainfall events (this fraction being subsequently
1067 available for direct evaporation) (Noilhan & Planton, 1989), while ETPART
1068 computes both potential vegetation transpiration and potential evaporation on
1069 soil, using a partition coefficient depending on LAI and a Beer-Lambert law
1070 (Huygen *et al.*, 1997). ROLI computes the actual amount of water extracted
1071 by roots in the soil according to the potential transpiration and the available
1072 water content (Li *et al.*, 2001). The root extraction computed by ROLI is a
1073 sink term in the Richards equation solved by FRER1D.

1074